Sensors & Actuators: B. Chemical 345 (2021) 130406

Contents lists available at ScienceDirect

Sensors and Actuators: B. Chemical

journal homepage: www.elsevier.com/locate/snb

A gated material as immunosensor for in-tissue detection of IDH1-R132H mutation in gliomas

Luis Pla [a,b,c], Félix Sancenón [a,b,c,d,e], M. Carmen Martínez-Bisbal [a,b,c,d,f,*], Ricardo Prat-Acín [c,g,h], Inmaculada Galeano-Senabre [c,g], Marina Botello-Marabotto [b,c], Sarai Palanca-Suela [i], Elena Aznar [a,b,c,d,e], Sara Santiago-Felipe [a,b,c,*], Ramón Martínez-Máñez [a,b,c,d,e,*]

[a] CIBER de Bioingeniería, Biomateriales y Nanomedicina (CIBER-BBN), Spain
[b] Instituto Interuniversitario de Investigación de Reconocimiento Molecular y Desarrollo Tecnológico, Universitat Politècnica de València, Universitat de València, Camino de Vera s/n, 46022, Valencia, Spain
[c] Unidad Mixta de Investigación en Nanomedicina y Sensores, Universitat Politècnica de València, Instituto de Investigación Sanitaria La Fe (IISLAFE), Valencia, Spain
[d] Unidad Mixta UPV-CIPF de Investigación en Mecanismos de Enfermedades y Nanomedicina. Universitat Politècnica de València, Centro de Investigación Príncipe Felipe, Valencia, Spain
[e] Departamento de Química, Universitat Politècnica de València, Valencia, Spain
[f] Departamento de Química Física, Universitat de València, Burjasot, Valencia, Spain
[g] Servicio de Neurocirugía, Hospital Universitario y Politécnico La Fe, Valencia, Spain
[h] Departamento de Cirugía, Universitat de València, Valencia, Spain
[i] Unidad de Biología Molecular, Servicio de Análisis Clínicos, Hospital Universitari i Politècnic La Fe, Valencia, Spain

ARTICLE INFO

Keywords:
Glioblastoma
Nanoporous anodic alumina
Gated material
Antibody
IDH1

ABSTRACT

A nanodevice consisted on nanoporous anodic alumina (NAA) supports functionalized with specific and selective antibody-based gatekeepers for the detection of IDH1-R132H mutant enzyme is here reported. Molecular profile and tissue mutations of the tumours (such as IDH1/IDH2 mutations in gliomas) are a great source of information that already make a difference in terms of prognosis and prediction of response to combined therapy. However, standardized methodologies to determine this mutation are time-consuming and cannot provide information before or during surgical intervention, which significantly limits their utility in terms of intraoperative decision-making. To solve this limitation, our sensing system, in the presence of the target IDH1-R132H mutant enzyme triggers the delivery of a fluorescent reporter from the antibody-capped NAA that is easily detected using a standard fluorimeter in less than 1 h. Good capabilities of the sensor in terms of sensitivity (limit of detection as low as 0.01 ng/mL) and selectivity are determined. The biosensor is validated in seventeen human glioma tissue samples, also analysed by standardized methodologies, showing significant differences between IDH1 wild-type and IDH1-R132H mutant gliomas ($p < 0.01$) with high sensitivity, specificity and accuracy (87.5/88.9/88.2) for IDH1-R132H mutational status classification in human glioma tissues. This new detection system might play an important role in surgical interventions, anticipating mutational status information in gliomas and supporting thus decision making and patient survival.

1. Introduction

Brain gliomas are a group of CNS (central nervous system) tumours, derived from glial cells. They may result in a wide range of tumours, including glioblastoma (GB), which is one of the most aggressive cancer diseases. Gliomas are categorized into four grades (I, II, III and IV) [1] according their aggressiveness, being grade IV or GB the most frequent and aggressive with a median survival of 15 months, despite standard therapy consistent in a combination of extensive surgery with concomitant radiotherapy and temozolomide [2–4]. Surgery plays an important role in the management of these tumours and it has been demonstrated that extent of resection is linked to increased survival. However, infiltrative nature of gliomas makes extremely difficult to obtain complete resections without significant morbidity. Unlike radiotherapy and

* Corresponding authors at: Instituto Interuniversitario de Investigación de Reconocimiento Molecular y Desarrollo Tecnológico, Universitat Politècnica de València, Universitat de València, Camino de Vera s/n, 46022, Valencia, Spain.
E-mail addresses: carmen.martinez-bisbal@uv.es (M.C. Martínez-Bisbal), sasanfe@upvnet.upv.es (S. Santiago-Felipe), rmaez@qim.upv.es (R. Martínez-Máñez).

https://doi.org/10.1016/j.snb.2021.130406
Received 14 April 2021; Received in revised form 1 July 2021; Accepted 2 July 2021
Available online 6 July 2021

chemotherapy, brain glioma surgery takes place without final pathological diagnosis, including molecular biology of the tumour. However, intraoperative knowledge of the mutational profile of the tumour could support a more aggressive or conservative surgical approach. Additionally, given the fateful effects associated with both the disease and treatments, it is important to develop diagnostic methods that allow and facilitate the detection and identification of these gliomas in their earliest, and therefore, least dangerous stages. In this scenario, it has been demonstrated a correlation between the presence of the R132H mutated enzyme isocitrate dehydrogenase 1 (IDH1) and a better prognosis in gliomas, thus becoming this mutant enzyme a recurrent biomarker for favourable prognosis of patients with grade III and IV gliomas, as well as a selective marker for the differentiation of so-called secondary GB from primary GB [1,5–7].

IDH1 is part of a group of enzymes involved in metabolic catalysis of isocitrate decarboxylation into α-ketoglutarate [6]. In 2008, the GB Cancer Genome Atlas project observed recurrent mutations at codon R132 in approximately 60–80 % of diffusely infiltrating gliomas [8]. The most habitual mutation detected was R132H (89.7 %), but other mutations have also been reported, for example R132C (2.8 %), R132 K (2.8 %), R132S (1.4 %) and R132 G (1.1 %) [9]. To date, this potential biomarker has been detected by routine clinical analysis such as direct sequencing [10,11], western-blot [12] and immunohistochemistry in tumour tissue using different anti-IDH1 (R132 H) antibodies [13–15]. Although some of them present high accuracy, these techniques are time consuming and require complex and expensive equipment [16]. Moreover, accuracy of immunohistochemistry assays, may be highly dependent on the technician expertise. In addition, and most important, the information provided by these sophisticated techniques is supplied after surgery, and therefore is not available for supporting intraoperative decision-making. In this scenario, rapid, cost-competitive, easy to handle, transportable and accurate detection systems are demanded for their implementation as close as possible to the surgery room, as an innovative and complementary tool in the intraoperative management of GB.

In this regard, nanotechnology may provide the tools for a valuable improvement of the current methodologies. Nowadays, examples of nano-resources for improving GB prognosis are few and rare. One of the examples, reported by H. Shao and collaborators [17], developed a microfluidic chip for target-specific labelling of microvesicles shed into circulation from GB, that were detected by a miniaturized nuclear magnetic resonance system. They provided good sensibility and selectivity results, but the technology employed is complex and expensive.

From another viewpoint, mesoporous materials, especially silica and alumina mesoporous materials, have been employed in plenty of innovative detection systems in the last decade [18]. In particular, the potential of nanoporous anodic alumina (NAA) in the design of biosensors has been shown owing the singular set of chemical, mechanical, optical, electrical and transport properties, including thermal stability, chemical resistance, hardness, large surface area and biocompatibility [19,20]. NAA is Al self-ordered porous metal oxide made with an electrochemical anodization [19]. By this process highly-ordered, vertically-aligned nanoporous and nanotubular structures with well-defined and controllable geometry, are successfully generated [20]. Hence it is a low cost and durable platform which enables an easy functionalization inside and outside the channels with different biomolecules as antibodies, aptamers, genes, peptides and enzymes [19–24]. Moreover, the combination of mesoporous materials with molecular gates (also known as gatekeepers or nanovalves) has resulted in the development of materials for sensing (such as pathogens [18,25–28], drug delivery [28–30]) and communication protocols [31,32]. In gated materials for sensing applications, the molecular gate effectively inhibits the delivery of the loaded reporter (usually a fluorophore) from the mesoporous support until the presence of a certain analyte. In this situation, usually a displacement of the gatekeeper takes place, allowing delivery of the loaded reporter to the solution. This sensing concept enables a host-guest interaction independent from the signalling unit, what provides an amplifying effect since few target analyte molecules are able to release a large quantity of entrapped signalling molecules [33,34]. As gatekeepers in gated materials for sensing applications different organic molecules, polymers, DNA, enzymes, nanoparticles and antibodies have been reported. Since the first proof of concept on the use of antibodies as gatekeepers for sensing applications [35], several silica-based gated materials employing antibodies for the recognition of organic small molecules such as finasteride [36], sulfathiazole [35] or explosives [37] have been reported. The design of molecular gates combining antibodies with other nanoscopic elements has also been reported, such as polystyrene nanoparticles for the detection of brevetoxin B [38], or polyethylenimine (PEI) and gold nanoparticles (AuNPs) for the detection of mycotoxins [39,40]. All of them show good results in terms of sensitivity and specificity. In our group, NAA supports have been combined previously with DNA molecular gates for the detection of bacteria [41] and recently with aptamers for sensing a protein as gliadin [42] for gluten detection in food, and for sensing an oncomarker in urine and serum as 8-oxo-dG [43] for sensing colonic cancer. These systems have shown very competitive sensitivity and specificity in complex media. Nevertheless, the detection of a mutant enzyme as IDH1-R132H requires a highly specific interaction of the molecular gate to exclusively act in the presence of the mutant enzyme and not in the presence of the wild-type enzyme. In this scenario, antibodies might serve as molecular gates to discriminate this mutation.

Based on the above, we report herein the design, preparation, characterization and validation of a new intra-surgical antibody-gated NAA sensing device for the detection of the IDH1-R132H mutant enzyme in gliomas, which is of remarkable interest as a prognosis tool in GB treatment. We use an anti-IDH1 (R132 H) antibody, a mouse monoclonal clone HMab-1 purified from hybridoma cell culture, as gatekeeper, being the first time that NAA is combined with antibodies working as molecular gates. The sensor is validated in seventeen human glioma samples resulting in significant differences between IDH1 wild-type and IDH1-R132H mutant glioma tissues ($p < 001$). The sensor shows high sensitivity, specificity and accuracy (87.5/88.9/88.2) for IDH1-R132H mutational status classification in human gliomas, with experimental requirements easy to implement by side the surgery room, and fast enough to support intraoperatory mutational diagnosis.

2. Materials and methods

2.1. General techniques

A ZEISS Ultra 55 microscope was employed to perform Field Emission Scanning Electron Microscopy (FESEM) and Energy Dispersive X-ray spectroscopy (EDX) analyses. Measurements of fluorescence spectroscopy were carried out on a Synergy H1 microplate reader (BioTek, Winooski, VT, USA). Brain tissues were homogenized with a T25 Digital Ultra Turrax homogenizer (IKA, Germany).

2.2. Chemicals

Protein isocitrate dehydrogenase (IDH1) wild-type and IDH1-R132H mutant enzyme standards were provided by Bionova Científica S.L. 3-(azidopropyl)triethoxysilane was provided by FluoroChem Ltd. Rhodamine B, tris(hydroxymethyl)aminomethane (TRIS), acetonitrile (CH_3CN), hydrochloric acid (HCl) and mouse monoclonal anti-IDH1-R132H antibody (clone HMab-1) were purchased from Sigma-Aldrich Química (Madrid, Spain). Propargyl glycine (Pra) derivatized peptide KPIIIGHHAYGD sequence was provided by Bionova Científica S.L. Copper (II) sulphate ($CuSO_4$) and sodium ascorbate ($C_6H_7O_6Na$) were supplied by Scharlab S.L.

2.3. NAA scaffolds

NAA scaffolds were purchased from InRedox (CO, USA). NAA consists of anodic aluminum oxide films grown on a 0.1 mm thick aluminum layer with a ca. 9×10^{11} cm^{-2} pore density. Pores in NAA are 10 μm deep and have a diameter of ca. 20−30 nm. As indicated by the manufacturer, the pore structure follows a funnel-like conformation with a diminishment of pore diameter from 20−30 nm in the entrances to 5 nm in the first 20 nm. After this transition, the pore diameter remains constant and uniform throughout a depth of 10 μm.

2.4. Synthesis of materials S1, S2 and S3

Gated materials synthesis may be divided in four separated stages: a) loading, b) functionalization, c) peptide anchoring and d) antibody capping. In a regular preparation, 10 new NAA supports of 2 mm of diameter were submerged in a rhodamine B solution in CH_3CN (8 mL, 1 mM) for 24 h at room temperature. Then, the surface was functionalized adding 3-(azidopropyl)triethoxysilane (5 μL per support) into a suspension of the supports in CH_3CN (1 mL) and rhodamine B (1 mM). The mixture was agitated for 6 h at room temperature, obtaining **S1**. Later, the alkyne-terminated peptide sequence KPIIIGHHAYGD-Pra (100 μg/mL) was added to a rhodamine-PBS 1x buffer solution with 5 individual **S1** supports. $CuSO_4$ (250 μL, 1 mM) and sodium ascorbate (250 μL, 10 mM) solutions in PBS 1x were added to the mixture. The cycloaddition reaction was run at 90 °C for 78 h to obtain **S2**. Finally, **S2** supports were submerged in 250 μL of a 5×10^{-5} mg/mL dilution of the commercial mouse monoclonal anti-IDH1-R132H antibody in PBS 1x buffer. The mixture was agitated 1 h at 25 °C and then, the supports were washed dropwise with PBS 1x buffer to give **S3**.

2.5. Assay protocol

Delivery of the entrapped indicator in the presence and in the absence of IDH1-R132H mutant enzyme, and in the presence of IDH1 wild-type enzyme was evaluated. For this, three independent **S3** supports were submerged separately in three plastic receptacles with PBS 1x buffer (1 mL, pH 7.4). IDH1-R132H mutant enzyme (100 μL, 1 μg/mL) was added to one of the solutions, the second solution was doped with IDH1 wild-type enzyme (100 μL, 1 μg/mL) and the third one was compensated with 100 μL of bare PBS 1x buffer. Mixtures were stirred at room temperature for 60 min and aliquots were taken periodically (every 15 min) for dye diffusion monitoring. Finally, fluorescence in the solution was measured at $\lambda_{ex/em} = 555/575$ nm for the whole set of aliquots. Assays were performed in duplicate.

2.6. Sensitivity and limit of detection (LOD)

Sensitivity of the sensor was tested studying the response of **S3** to decreasing concentrations of IDH1-R132H mutant enzyme, covering the range from 10^3 to 10^{-5} ng/mL. For this, eight separated **S3** were submerged in PBS 1x buffer solutions containing different concentrations of the mutant protein. Suspensions were mixed at room temperature for 60 min. Finally, dye diffusion to the solution was determined by fluorescence emission at $\lambda_{ex/em} = 555/575$ nm. Assays were performed in duplicate.

Sensitivity studies in realistic media were tested studying the response of **S3** to decreasing concentrations of IDH1-R132H mutant enzyme in brain tissue homogenized samples. For that, 250 μL of homogenized samples lacking mutant protein were artificially inoculated with with serial dilutions of IDH1-R132H mutant enzyme ranging from 10^2 to 10^{-9} ng/mL and added to nine separated **S3** supports in a final volume of 400 μL with PBS 1x buffer. Suspensions were stirred at room temperature for 60 min. Finally, dye diffusion to the solution was determined by fluorescence at $\lambda_{ex/em} = 555/575$ nm. Experiments were carried out twice. OriginPro Version 9 (OriginLab Corporation, Northampton, MA, USA) was used to fit the LOD data to a sigmoidal curve using a Boltzmann function.

2.7. Tissue samples

The present study was approved by the Ethics Committee of Hospital Universitari i Politècnic La Fe (2019/0108), Valencia, Spain. Patients were recruited from Neurosurgery service in Hospital Universitari i Politècnic La Fe. Seventeen adult patients with histopathological diagnosis of brain glioma were included in the study and gave informed consent. In the surgical procedure, two small tissue aliquots from each patient were preserved in RNAlater solution and afterwards they were stored at -80 °C by the Biobanco La Fe (PT13/0010/0026) in the Instituto de Investigación Sanitaria La Fe, until the moment of analysis. From the two aliquots preserved, one of them was used to test the new sensing system and the other aliquot underwent routine histological analysis and mutational status determination, according to the standardized protocols.

Paired Formalin-Fixed Paraffin-Embedded (FFPE) GB tissue samples were retrieved from the tissue archives of the Departments of Pathology of the Hospital Universitari i Politècnic La Fe. Tissue sections were macrodissected by a pathologist to select regions containing the highest proportion of tumour cells. Only samples with at least 50 % of tumoral cells were selected to DNA isolation. Genomic DNA was isolated from five 5-μm thick FFPE sections using Deparaffinization Solution and QIAamp DNA Investigator Kit (Qiagen, Hilden, Germany) according to manufacturer's protocol. DNA concentration was quantified by Qubit dsDNA HS Assay Kit (ThermoFisher Scientific) and mutational status of the IDH1 [LRG_610 (t1) NM_005896.3] gene was determined by PCR and Sanger sequencing. Target sequences were amplified using pairs of primers previously described [44–46]. For loci R132 (exon 4 of the IDH1 gene) reaction (total volume of 25.0 μL) contained 2.0 μL of DNA (50 ng/μL), 12.5 μL of Type-it Multiplex PCR Master Mix (2x), 2.5 μL of Q-Solution (5x), 7.0 μL of DNase/RNase-free H_2O, and 0.5 μL primer mix (concentration of 10 μM). The PCR was performed in a conventional thermal cycler using the following cycling conditions: initial heating at 95 °C for 5 min followed by 40 cycles of 45 s denaturation at 95 °C, 45 s annealing at 59 °C, 60 s extension at 72 °C, and, finally, 72 °C for 10 min. PCR product was subsequently sequenced on the ABIprism 3130 (Applied Biosystems). The other tissue aliquot was prepared to test the new sensing system. Samples were thawed, suspended in PBS 1x buffer (2 mL) and homogenized employing an Ultra Turrax homogenizer. Then, homogenized samples were stored at -80 °C until their analysis.

2.8. Validation of S3 nanodevice in brain tissue samples

A set of seventeen glioma tissue samples from patients of Hospital Universitari i Politècnic La Fe of Valencia were tested to stablish the diagnosis capacity of the developed biosensor. For that, 250 μL of each homogenized tissue suspension were diluted in 150 μL of PBS 1x buffer and an individual **S3** support was incorporated. Suspensions were stirred for 60 min at room temperature and the aliquots were obtained at the beginning and at the end of the assays. Finally, rhodamine B dye delivery was measured by fluorescence spectroscopy at $\lambda_{ex/em} = 555/575$ nm. These validation experiments were performed in triplicate for each of the seventeen samples. Average fluorescence measured at 60 min of the three experiments was calculated for each sample. Non-parametric U-Mann-Whitney test was used to assess the significance of differences between response of **S3** to IDH1 wild-type and IDH1-R132H mutant gliomas. The AUC (area under curve) ROC (receiver-operating characteristic) was calculated to determine the diagnostic ability of **S3** as classifier for IDH1-R132H mutational status. U-Mann-Whitney test and AUC - ROC curve analyses were performed using GraphPad Prism version 8.0.1 for Windows (GraphPad Software, San Diego, California USA).

3. Results and discussion

3.1. Gated material preparation and characterization

The preparation of the gated biosensor was carried out in several steps (Scheme 1). First, NAA supports (**S0**) were loaded with the fluorescent indicator rhodamine B. Then, the surface of the support was azide-functionalized (**S1**) and the surface of **S1** was reacted with an alkyne derivatized peptide sequence (Pra-KPIIIGHHAYGD) through a Huisgen cycloaddition reaction [47,48] to obtain **S2**. The peptide sequence has previously been used as an antigen [49] for the generation of antibodies (mIDH1R132 H), and as a linker for anchoring the corresponding antibody in ELISA assays [50], being thus a good candidate for linking the antibody to the nanoporous material in our design. In a final step, **S2** supports were submerged in a solution of the anti-IDH1-R132H antibody in PBS 1x buffer. The antibody interaction with the peptide results in pore capping, giving the final biosensor **S3**. **S3** is expected to be capped due to the bulky antibody, whereas the presence of the mutant IDH1-R132H mutant enzyme should selectively induce antibody displacement and cargo release (Scheme 2).

S0, **S1**, **S2** and **S3** were characterized by FESEM and EDX analyses. The porous surface of NAA scaffolds can be observed in Fig. 1a. FESEM images from **S3** show an organic layer attributed to the presence of organic matter in the successive functionalization steps and the capping antibody. Moreover, these images also show the presence of small areas of uncovered pores, which demonstrates that the nanoporous structure remained unaltered despite the consecutive chemical reactions performed on the surface for the mesoporous support functionalization and capping (area marked in Fig. 1b).

Through the study and surface composition analysis of each one of the synthesized materials it was possible to follow the different synthetic steps. Energy dispersive X-ray spectroscopy (Table 1) shows a high C content (C/Al 1.11) for **S1** due to the presence of rhodamine B. Also, a significant silicon and nitrogen content is found as consequence of the superficial 3-azidopropylthrietoxysilane functionalization. **S2** and **S3** showed a decrease of carbon content attributed to a partial release of the indicator during the capping processes. Moreover, a remarkable increase in N and S atoms are observed in **S3** when compared with **S2**, which is in agreement with the presence of the antibody as capping system in **S3**.

3.2. Diagnostic performance

In a first step the performance of the antibody-capped **S3** biosensor was tested in the presence and in the absence of the target IDH1-R132H mutant enzyme, and in the presence of the IDH1 wild-type enzyme following the procedures explained in the 2.5 section. In the presence of the IDH1-R132H mutant enzyme the capping antibody is displaced resulting in pore opening and spreading the encapsulated dye (detected by fluorescence spectroscopy) (Fig. 2). In contrast, cargo delivery was significantly less remarkable in the presence of the native protein and in the control experiment (bare PBS 1x buffer). Despite being observed a maximum of cargo delivery at 60 min, a similar difference was already observed at 45 min, and also evident differences were found at 30 and 15 min, in the presence of IDH1-R132H mutant enzyme when compared with the blank and the IDH1 wild-type enzyme (Fig. 2). This enables a time of response in the detection of IDH1-R132H mutant enzyme in less than 1 h. Despite the affinity of the peptide for the anti-IDH1-R132H antibody used as gatekeeper [13], the results demonstrate that the presence of IDH1-R132H mutant enzyme induces antibody displacement and payload delivery (Scheme 2). Thus, this novel combination of NAA with antibody gatekeepers demonstrates to be useful for sensing the mutated enzyme.

3.3. Sensitivity, specificity studies and robustness

Considering that the purpose of **S3** is providing support for diagnostic, it is of main importance to determine its sensitivity and specificity. With this purpose, the response of **S3** in the presence of increasing concentrations of IDH1-R132H mutant enzyme was evaluated. As observed in Fig. 3a, an almost linear response proportional to the concentration of mutant protein was observed in the 100 to 0.01 ng/mL range and a LOD as low as 0.01 ng/mL was determined. This LOD was established according to the change in sensor response for different concentration ranges (10^{-4} to 10^{-2} ng/mL and 10^{-2} to 100 ng/mL; Fig. 3). Analogously, and in order to evaluate the effect of complex matrixes in the sensitivity of **S3** nanodevice, its response to different concentrations of IDH1-R132H mutant enzyme in homogenised brain tissues was studied. For that, nine brain tissue homogenised samples lacking IDH1-R132H mutant enzyme were artificially doped with different concentrations of mutant protein that ranged from 10^{-9} to 10^{2} ng/mL. Then, 250 µL of each sample was added to an Eppendorf tube containing the **S3** support and 150 µL of PBS 1x buffer. It was proved that the sensitivity was not significantly affected by the tissue matrix, and the LOD kept unaltered at 0.01 ng/mL (Fig. 3b).

In comparison with other reported antibody-based methodologies for the detection of the IDH1-R132H mutant enzyme, our system provides a higher sensitivity (0.01 ng/mL = 1×10^{-11} g/mL) with LOD five orders of magnitude lower than previously described methods. For example, Y. Fujii reported a LOD of 1 µg/mL (1×10^{-6} g/mL) for western-blot analyses run with HMab-1 and HMab-2 anti IDH1-R132H antibodies [13], while S. Takano reported a LOD of 5 µg/mL (5×10^{-6} g/mL) employing IMab-1 antibody [51]. Other researchers such as A. Yamamichi and collaborators, developed a microdevice for the detection of IDH1-R132H mutant enzyme with HMab-2 antibody, which showed a LOD of 0.5 mg/mL (5×10^{-4} g/mL) [16].

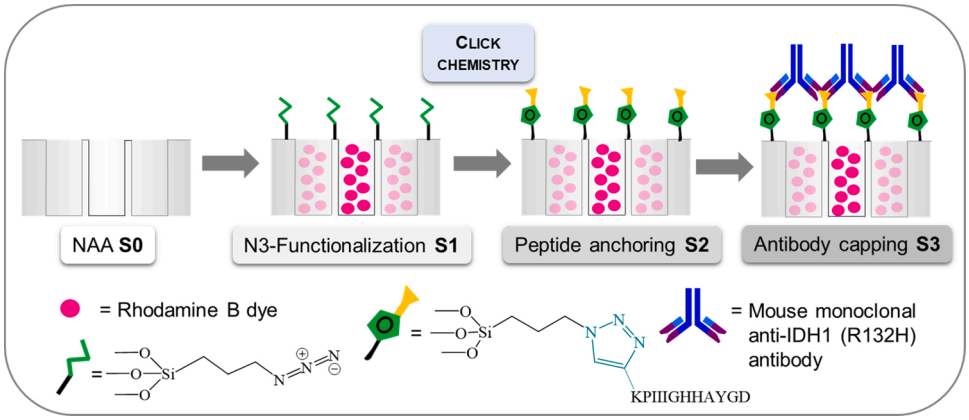

Scheme 1. Process for the preparation of the **S3** supports (loading, functionalization, peptide anchoring and antibody capping).

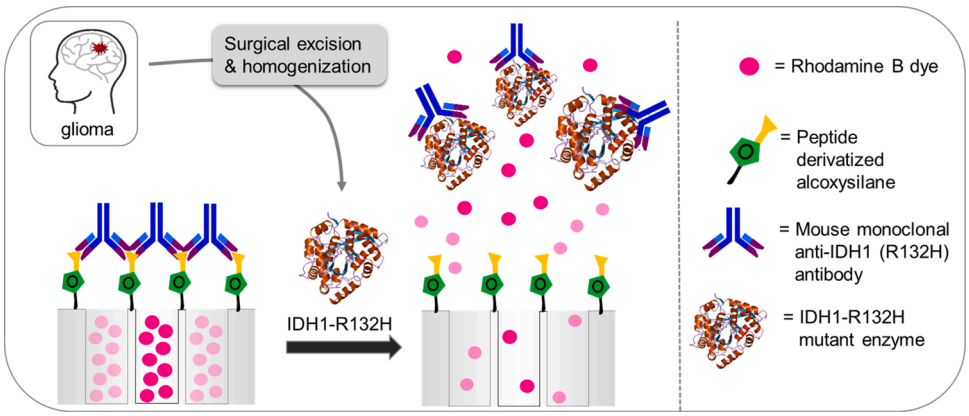

Scheme 2. Illustrative description of **S3** detection mechanism.

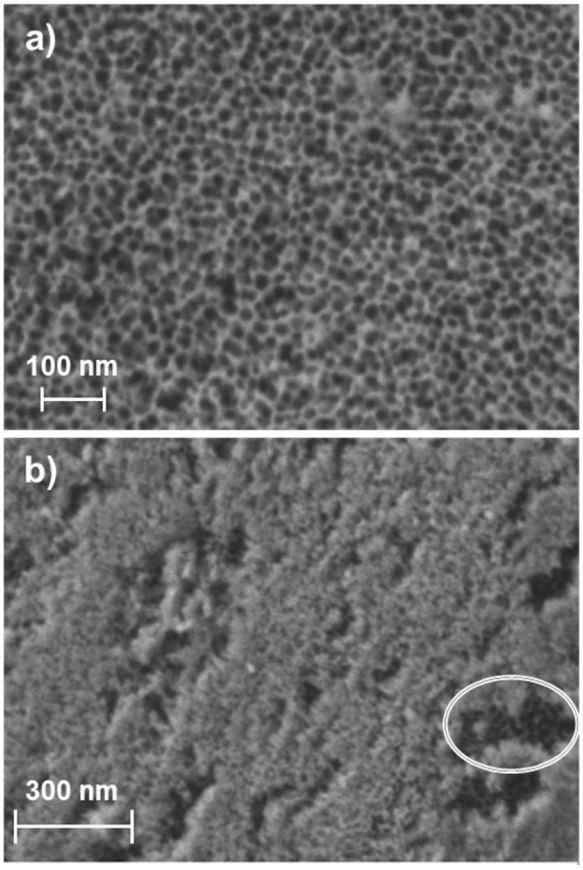

Fig. 1. FESEM images of (a) NAA and (b) **S3** supports.

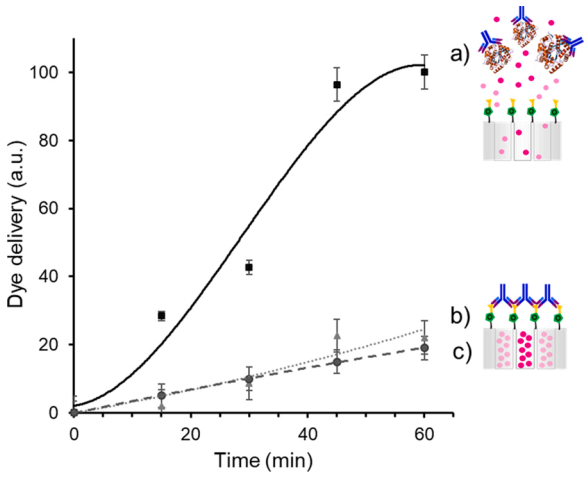

Fig. 2. Rhodamine B delivery profile of **S3** support a) in the presence of target IDH1-R132H mutant enzyme, b) in the absence of mutant protein (bare PBS 1x buffer) and c) in the presence of IDH1 wild-type enzyme.

Table 1
Atomic elements ratios to Al in the different prepared solids.

	C/Al	Si/Al	N/Al	S/Al
S1	1.11	0.13	0.03	–
S2	0.62	0.12	0.09	0.01
S3	0.59	0.14	0.12	0.20

3.4. IDH1-R132H mutant enzyme in clinical samples. Validation of the S3 biosensor

Validation of the **S3** biosensor was carried out in brain tissues surgically extracted from patients with and without IDH1-R132H mutant enzyme. After surgery, the tissues underwent routine histological analysis to determine type and grade of glioma. Moreover, the mutational status was determined in each sample as explained in the 2.7 section. The glioma type and grade, and IDH1-R132H mutational status for each analysed sample is shown Table 2. According to this, 8 gliomas presented the IDH-R132H mutation and 9 gliomas presented the IDH1 wild type enzyme.

Homogenized samples from brain tissue surgically extracted from patients with and without the IDH1-R132H mutant enzyme were diluted in PBS 1x buffer 1.5:1 ratio (homogenized sample:buffer), and then, independent **S3** supports were immersed in each of these solutions. After 60 min with agitation at room temperature, the fluorescence emission in the solution was recorded. Samples were analysed in triplicate. The average normalized fluorescence emission for each sample and the median (in red) is shown in the Fig. 4a for both groups; i.e. samples containing the native IDH1 or the IDH1-R132H mutant enzyme. U-Mann-Whitney test showed significant differences between both groups ($p = 0.0016$). As shown in Fig. 4a, average dye delivery values in IDH1-R132H-containing samples was more than twice the dye delivery in control samples (32 ± 24 *vs* 13 ± 7 a.u.). This analysis reveals a significant increment in the fluorescence signal using **S3** in brain tumours containing IDH1-R132H mutant enzyme related to brain tissue samples expressing IDH1 wild type enzyme. To assess the potential use of the nanosensor as a diagnostic tool to determine mutational status, we calculated the ROC curve to discriminate between tumour tissue that express the IDH1-R132H mutant enzyme or the IDH1 wild-type enzyme

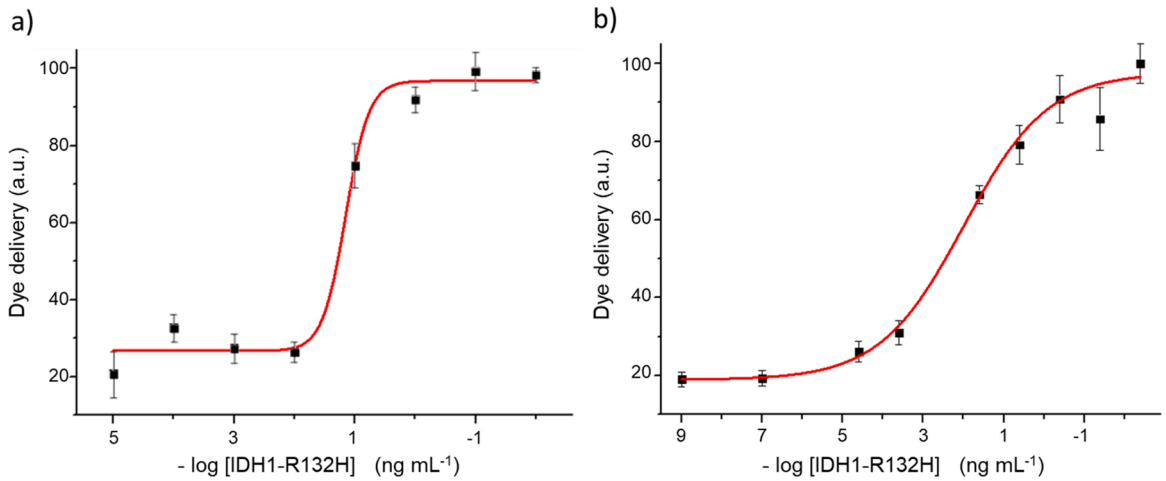

Fig. 3. Dye delivery recorded for different **S3** supports: a) immersed in PBS 1x buffer solutions doped with eight different and growing concentrations of IDH1-R132H mutant enzyme. LOD was stablished in 0.01 ng/mL. b) in brain tissue homogenized media doped with nine different concentrations of IDH1-R132H mutant enzyme. LOD was stablished in 0.01 ng/mL.

Table 2
Human glioma tumour tissue samples used for the validation of the S3 biosensor and analysed by routine clinical procedures to stablish type, grade of glioma and IDH1-R132H mutational status.

SAMPLE	Type	Grade	IDH1-R132H [a]
1	Oligodendroglioma	II	+
2	Diffuse astrocytoma	II	+
3	Diffuse oligodendroglioma	II	+
4	Glioblastoma	IV	–
5	Diffuse oligodendroglioma	II	+
6	Diffuse anaplastic glioma	III	+
7	Diffuse anaplastic glioma	II	+
8	Glioblastoma	IV	–
9	Glioblastoma	IV	–
10	Glioblastoma	IV	–
11	Glioblastoma	IV	+
12	Glioblastoma	IV	+
13	Glioblastoma	IV	–
14	Glioblastoma	IV	–
15	Glioblastoma	IV	–
16	Low-grade glioma	–	–
17	Glioblastoma	IV	–

a) Positive (+) means that IDH1-R132H mutant enzyme was determined in samples by molecular diagnosis and histopathology techniques standardized and accepted by the WHO.

(Fig. 4b). Particularly, **S3** biosensor ability to detect the presence of target IDH1-R132H mutant enzyme in glioma tissue homogenisates achieves 88 % of sensitivity, 89 % of specificity, and 88 % of accuracy using the optimal cut-off value of 18 and with an area under the curve of 0.9306, considering all glioma type and grade. These results show a good agreement with the data provided by routine analyses and good sensitivity and specificity to detect the IDH1-R132H mutant enzyme in glioma tissue.

Common methodology employed by hospitals to detect and identify IDH1-R132H mutant enzyme in tissue samples require several steps: 1) tissue section macrodissection by pathologists, 2) extraction and isolation of genomic DNA, 3) DNA concentration, 4) gene determination by PCR and Sanger sequencing and finally, 5) target DNA sequences amplification. Despite this technique provides high sensitivity and specificity, it usually requires long sample processing times (approximately 2 weeks) to provide the mutational status information and expensive and specialized equipment and staff. These factors hamper the application of these procedures as a quick diagnostic tool anticipating mutational status in surgical interventions. In contrast to this stablished methodology, our antibody-capped **S3** biosensor can be implemented as

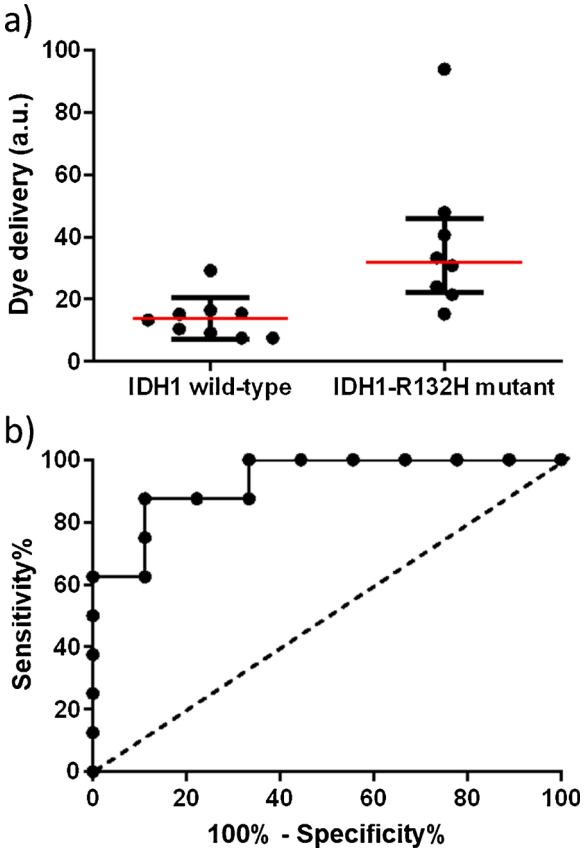

Fig. 4. a) **S3** support average response for the presence of IDH1 wild-type enzyme and IDH1-R132 mutant enzyme in human glioma samples analysed in triplicate. Fluorescence measurements were obtained at 60 min in homogenisates-PBS mixtures at pH 7.5. Data are represented as median + standard error; $p < 0.01$ when compared using U-Mann-Whitney test. b) ROC analysis displays the specificity and sensitivity of the developed sensor to discriminate between brain tissue samples with and without the IDH1-R132H mutant enzyme.

a point-of-care system: (i) it is fast and can provide results in less than 1 h; (ii) the required equipment to obtain a response is simple and common in most laboratories; (iii) the cost of preparation and testing is low comparing to other standardized techniques; (iv) sample pre-

treatments is reduced to simple homogenization; (v) it is easy to use and highly specialised staff is not required; and (vi) it allows the *in situ* analysis of samples in the surgery room itself or by side, providing fast information of great relevance to the neurosurgery team to support timely decision making.

Moreover, **S3** biosensor appears as a versatile tool to differentiate samples with IDH1-R132H mutant enzyme and independently of glioma grade and type. Given the implications of IDH1 mutational status in prognosis, point-of-care biosensors such as **S3** are relevant for all type of gliomas, but it is of the great importance in GB, since intraoperative knowledge of the mutational status could support a more aggressive or conservative surgical approach in these tumors, and make a difference in the patient survival.

4. Conclusions

Herein is reported a new in-tissue diagnosis tool for the detection of IDH1-R132H mutant enzyme, a biomarker for patients' prognosis, that could be of help in the decision-making during the surgical interventions of gliomas. The biosensor consists of a NAA support loaded with a fluorescent indicator, functionalized with a peptide and capped with an antibody. In the presence of the IDH1-R132H mutant enzyme, the antibody displaces from the support's surface and the indicator is delivered. The biosensor shows excellent results in terms of selectivity and sensitivity with a LOD as low as 0.01 ng/mL in buffer and in homogenized glioma tissues. This novel combination of NAA with antibodies as gatekeepers might serve as inspiration for the design of new systems aiming for the sensing of mutant enzymes in complex media. The system is successfully validated in seventeen glioma samples surgically extracted from patients with and without the IDH1-R132H mutant enzyme. The response using **S3** shows significant differences between IDH1 wild-type and IDH1-R132H mutant gliomas ($p < 0.01$) with high sensitivity, specificity and accuracy (87.5/88.9/88.2) for IDH1-R132H mutant enzyme detection in human glioma tissues. This or similar point-of-case biosensors could be of importance to support intraoperatory decision-making in the context of gliomas handling.

CRediT authorship contribution statement

Luis Pla: Investigation, Methodology, Formal analysis, Writing - original draft. **Félix Sancenón:** Investigation, Supervision. **M. Carmen Martínez-Bisbal:** Conceptualization, Formal analysis, Writing - review & editing. **Ricardo Prat-Acín:** Conceptualization, Resources, Funding acquisition, Writing - review & editing. **Inmaculada Galeano-Senabre:** Resources, Writing - original draft. **Marina Botello-Marabotto:** Investigation. **Sarai Palanca-Suela:** Investigation, Resources. **Elena Aznar:** Investigation, Methodology, Writing - review & editing. **Sara Santiago-Felipe:** Investigation, Methodology, Formal analysis, Writing - review & editing. **Ramón Martínez-Máñez:** Conceptualization, Supervision, Funding acquisition, Writing - review & editing.

Declaration of Competing Interest

The authors declare that they have no known competing financial interests or personal relationships that could have appeared to influence the work reported in this paper.

Acknowledgements

This study was supported by the Spanish Government (project RTI2018-100910-B-C41 MCUI/AEI/FEDER, UE), the Generalitat Valenciana (project PROMETEO/2018/024), the Universitat Politècnica de València–Instituto de Investigación Sanitaria La Fe (GLIOVIEW-IDH and GLIOVIEWIDH_2.0 project) and CIBER-BBN (NANOPATH AND CANDI-EYE projects). S.S. thanks the Instituto de Salud Carlos III and the European Social Fund for the financial support "Sara Borrell" (CD16/000237). L.P. thanks to Ministerio de Economia, Industria y Competitividad for his FPI grant. We also aknowledge service provided by Biobanco La Fe of Instituto de Investigación Sanitaria La Fe, València, Spain.

References

[1] D.N. Louis, A. Perry, G. Reifenberger, A. von Deimling, D. Figarella-Branger, W. K. Cavenee, H. Ohgaki, O.D. Wiestler, P. Kleihues, D.W. Ellison, The 2016 World Health Organization Classification of Tumors of the Central Nervous System: a summary, Acta Neuropathol. 131 (2016) 803–820, https://doi.org/10.1007/s00401-016-1545-1.

[2] B.M. Alexander, T.F. Cloughesy, Adult glioblastoma, J. Clin. Oncol. 35 (2017) 2402–2409, https://doi.org/10.1200/JCO.2017.73.0119.

[3] R. Stupp, W.P. Mason, M.J. van den Bent, M. Weller, B. Fisher, M.J.B. Taphoorn, K. Belanger, A.A. Brandes, C. Marosi, U. Bogdahn, J. Curschmann, R.C. Janzer, S. K. Ludwin, T. Gorlia, A. Allgeier, D. Lacombe, J.G. Cairncross, E. Eisenhauer, R. O. Mirimanoff, Radiotherapy plus concomitant and adjuvant temozolomide for glioblastoma, N. Engl. J. Med. 352 (2005) 987–996, https://doi.org/10.1056/NEJMoa043330.

[4] R. Stupp, M.E. Hegi, W.P. Mason, M.J. van den Bent, M.J. Taphoorn, R.C. Janzer, S. K. Ludwin, A. Allgeier, B. Fisher, K. Belanger, P. Hau, A.A. Brandes, J. Gijtenbeek, C. Marosi, C.J. Vecht, K. Mokhtari, P. Wesseling, S. Villa, E. Eisenhauer, T. Gorlia, M. Weller, D. Lacombe, J.G. Cairncross, R.O. Mirimanoff, Effects of radiotherapy with concomitant and adjuvant temozolomide versus radiotherapy alone on survival in glioblastoma in a randomised phase III study: 5-year analysis of the EORTC-NCIC trial, Lancet Oncol. 10 (2009) 459–466, https://doi.org/10.1016/S1470-2045(09)70025-7.

[5] M. Megova, J. Drabek, V. Koudelakova, R. Trojanec, O. Kalita, M. Hajduch, *Isocitrate dehydrogenase 1* and *2* mutations in gliomas, J. Neurosci. Res. 92 (2014) 1611–1620, https://doi.org/10.1002/jnr.23456.

[6] M.S. Waitkus, B.H. Diplas, H. Yan, Isocitrate dehydrogenase mutations in gliomas, Neuro. Oncol. 18 (2016) 16–26, https://doi.org/10.1093/neuonc/nov136.

[7] L. Xia, B. Wu, Z. Fu, F. Feng, E. Qiao, Q. Li, C. Sun, M. Ge, Prognostic role of IDH mutations in gliomas: a meta-analysis of 55 observational studies, Oncotarget 6 (2015) 17354–17365, https://doi.org/10.18632/oncotarget.4008.

[8] K.M. Kurian, H.R. Haynes, C. Crosby, K. Hopkins, M. Williams, IDH mutation analysis in gliomas as a diagnostic and prognostic biomarker, Br. J. Neurosurg. 27 (2013) 442–445, https://doi.org/10.3109/02688697.2013.771139.

[9] H. Arita, Y. Narita, A. Yoshida, N. Hashimoto, T. Yoshimine, K. Ichimura, IDH1/2 mutation detection in gliomas, Brain Tumor Pathol. 32 (2015) 79–89, https://doi.org/10.1007/s10014-014-0197-x.

[10] M. Andrulis, D. Capper, T. Luft, C. Hartmann, H. Zentgraf, A. von Deimling, Detection of isocitrate dehydrogenase 1 mutation R132H in myelodysplastic syndrome by mutation-specific antibody and direct sequencing, Leuk. Res. 34 (2010) 1091–1093, https://doi.org/10.1016/j.leukres.2010.02.014.

[11] W.C. Goh, B. Idris, R. Kandasamy, S. Shamsuddin, H. Jaafar, F. Ahmad, PCR-RFLP method enhance DNA sequencing of IDH1 somatic mutations detection in gliomas, GULHANE Med. J. 61 (2019) 167–171, https://doi.org/10.26657/gulhane.00078.

[12] D. Capper, H. Zentgraf, J. Balss, C. Hartmann, A. Von Deimling, Monoclonal antibody specific for IDH1 R132H mutation, Acta Neuropathol. 118 (2009) 599–601, https://doi.org/10.1007/s00401-009-0595-z.

[13] Y. Fujii, S. Ogasawara, H. Oki, X. Liu, M.K. Kaneko, S. Takano, Y. Kato, A high-sensitive HMab-2 specifically detects IDH1-R132H, the most common IDH mutation in gliomas, Biochem. Biophys. Res. Commun. 466 (2015) 733–739, https://doi.org/10.1016/j.bbrc.2015.09.070.

[14] D.D. Gondim, M.A. Gener, K.L. Curless, A.A. Cohen-Gadol, E.M. Hattab, L. Cheng, Determining IDH-Mutational status in gliomas using IDH1-R132H antibody and polymerase chain reaction, Appl. Immunohistochem. Mol. Morphol. 27 (2019) 722–725, https://doi.org/10.1097/PAI.0000000000000702.

[15] V. Sipayya, I. Sharma, K.C. Sharma, A. Singh, Immunohistochemical expression of IDH1 in gliomas: a tissue microarray-based approach, J. Cancer Res. Ther. 8 (2012) 598–601, https://doi.org/10.4103/0973-1482.106567.

[16] A. Yamamichi, T. Kasama, F. Ohka, H. Suzuki, A. Kato, K. Motomura, M. Hirano, M. Ranjit, L. Chalise, M. Kurimoto, G. Kondo, K. Aoki, N. Kaji, M. Tokeshi, T. Matsubara, T. Senga, M.K. Kaneko, H. Suzuki, M. Hara, T. Wakabayashi, Y. Baba, Y. Kato, A. Natsume, An immuno-wall microdevice exhibits rapid and sensitive detection of IDH1-R132H mutation specific to grade II and III gliomas, Sci. Technol. Adv. Mater. 17 (2016) 618–625, https://doi.org/10.1080/14686996.2016.1227222.

[17] H. Shao, J. Chung, L. Balaj, A. Charest, D.D. Bigner, B.S. Carter, F.H. Hochberg, X. O. Breakefield, R. Weissleder, H. Lee, Protein typing of circulating microvesicles allows real-time monitoring of glioblastoma therapy, Nat. Med. 18 (2012) 1835–1840, https://doi.org/10.1038/nm.2994.

[18] F. Sancenón, L. Pascual, M. Oroval, E. Aznar, R. Martínez-Máñez, Gated silica mesoporous materials in sensing applications, ChemistryOpen 4 (2015) 418–437, https://doi.org/10.1002/open.201500053.

[19] M.A. Tabrizi, J. Ferré-Borrull, L.F. Marsal, Advances in optical biosensors and sensors using nanoporous anodic alumina, Sensors 20 (2020) 5068, https://doi.org/10.3390/s20185068.

[20] A. Santos, T. Kumeria, D. Losic, Nanoporous anodic aluminum oxide for chemical sensing and biosensors, TrAC - Trends Anal. Chem. 44 (2013) 25–38, https://doi.org/10.1016/j.trac.2012.11.007.

[21] C. Eckstein, L.K. Acosta, L. Pol, E. Xifré-Pérez, J. Pallares, J. Ferré-Borrull, L. F. Marsal, Nanoporous anodic alumina surface modification by electrostatic, covalent, and immune complexation binding investigated by capillary filling, ACS Appl. Mater. Interfaces 10 (2018) 10571–10579, https://doi.org/10.1021/acsami.8b00572.
[22] M. Amouzadeh Tabrizi, J. Ferré-Borrull, L.F. Marsal, Highly sensitive aptasensor based on interferometric reflectance spectroscopy for the determination of amyloid β as an Alzheimer's disease biomarkers using nanoporous anodic alumina, Biosens. Bioelectron. 137 (2019) 279–286, https://doi.org/10.1016/j.bios.2019.04.050.
[23] A. Santos, G. MacÍas, J. Ferré-Borrull, J. Pallarès, L.F. Marsal, Photoluminescent enzymatic sensor based on nanoporous anodic alumina, ACS Appl. Mater. Interfaces 4 (2012) 3584–3588, https://doi.org/10.1021/am300648j.
[24] M. Nemati, A. Santos, T. Kumeria, D. Losic, Label-free real-time quantification of enzyme levels by interferometric spectroscopy combined with gelatin-modified nanoporous anodic alumina photonic films, Anal. Chem. 87 (2015) 9016–9024, https://doi.org/10.1021/acs.analchem.5b02225.
[25] L. Pla, E. Xifré-Pérez, À. Ribes, E. Aznar, M.D. Marcos, L.F. Marsal, R. Martínez-Máñez, F. Sancenón, A *Mycoplasma* genomic DNA probe using gated nanoporous anodic alumina, Chempluschem 82 (2017) 337–341, https://doi.org/10.1002/cplu.201600651.
[26] L. Pla, S. Santiago-Felipe, M.Á. Tormo-Mas, J. Pemán, F. Sancenón, E. Aznar, R. Martínez-Máñez, Aptamer-capped nanoporous anodic alumina for Staphylococcus aureus detection, Sens. Actuators B Chem. 320 (2020) 128281, https://doi.org/10.1016/j.snb.2020.128281.
[27] E. Aznar, M. Oroval, L. Pascual, J.R. Murguía, R. Martínez-Máñez, F. Sancenón, Gated materials for on-command release of guest molecules, Chem. Rev. 116 (2016) 561–718, https://doi.org/10.1021/acs.chemrev.5b00456.
[28] E. Aznar, R. Villalonga, C. Giménez, F. Sancenón, M.D. Marcos, R. Martínez-Máñez, P. Díez, J.M. Pingarrón, P. Amorós, Glucose-triggered release using enzyme-gated mesoporous silica nanoparticles, Chem. Commun. 49 (2013) 6391–6393, https://doi.org/10.1039/c3cc42210k.
[29] A. García-Fernández, E. Aznar, R. Martínez-Máñez, F. Sancenón, New advances in in vivo applications of gated mesoporous silica as drug delivery nanocarriers, Small 16 (2020) 1902242, https://doi.org/10.1002/smll.201902242.
[30] A. Llopis-Lorente, B. Lozano-Torres, A. Bernardos, R. Martínez-Máñez, F. Sancenón, Mesoporous silica materials for controlled delivery based on enzymes, J. Mater. Chem. B 5 (2017) 3069–3083, https://doi.org/10.1039/c7tb00348j.
[31] A. Llopis-Lorente, P. DÍez, A. Sánchez, M.D. Marcos, F. Sancenón, P. Martínez-Ruiz, R. Villalonga, R. Martínez-Máñez, Interactive models of communication at the nanoscale using nanoparticles that talk to one another, Nat. Commun. 8 (2017) 1–7, https://doi.org/10.1038/ncomms15511.
[32] B. Luis, A. Llopis-Lorente, P. Rincón, J. Gadea, F. Sancenón, E. Aznar, R. Villalonga, J.R. Murguía, R. Martínez-Máñez, An interactive model of communication between abiotic nanodevices and microorganisms, Angew. Chemie Int. Ed. 58 (2019) 14986–14990, https://doi.org/10.1002/anie.201908867.
[33] M. Hecht, E. Climent, M. Biyikal, F. Sancenón, R. Martínez-Máñez, K. Rurack, Gated hybrid delivery systems: en route to sensory materials with inherent signal amplification, Coord. Chem. Rev. 257 (2013) 2589–2606, https://doi.org/10.1016/j.ccr.2013.03.020.
[34] À. Ribes, E. Aznar, S. Santiago-Felipe, E. Xifre-Perez, M. ángeles Tormo-Mas, J. Pemán, L.F. Marsal, R. Martínez-Máñez, Selective and sensitive probe based in oligonucleotide-capped nanoporous alumina for the rapid screening of infection produced by Candida albicans, ACS Sens. 4 (2019) 1291–1298, https://doi.org/10.1021/acssensors.9b00169.
[35] E. Climent, A. Bernardos, R. Martínez-Máñez, A. Maquieira, M.D. Marcos, N. Pastor-Navarro, R. Puchades, F. Sancenón, J. Soto, P. Amorós, Controlled delivery systems using antibody-capped mesoporous nanocontainers, J. Am. Chem. Soc. 131 (2009) 14075–14080, https://doi.org/10.1021/ja904456d.
[36] E. Climent, R. Martínez-Máñez, Á. Maquieira, F. Sancenón, M.D. Marcos, E. M. Brun, J. Soto, P. Amorós, Antibody-capped mesoporous nanoscopic materials: design of a probe for the selective chromo-fluorogenic detection of finasteride, ChemistryOpen 1 (2012) 251–259, https://doi.org/10.1002/open.201100008.
[37] E. Climent, M. Biyikal, D. Gröninger, M.G. Weller, R. Martínez-Máñez, K. Rurack, Multiplexed detection of analytes on single test strips with antibody-gated indicator-releasing mesoporous nanoparticles, Angew. Chemie Int. Ed. 59 (2020) 23862–23869, https://doi.org/10.1002/anie.202009000.
[38] B. Zhang, B. Liu, J. Liao, G. Chen, D. Tang, Novel electrochemical immunoassay for quantitative monitoring of biotoxin using target-responsive cargo release from mesoporous silica nanocontainers, Anal. Chem. 85 (2013) 9245–9252, https://doi.org/10.1021/ac4019878.
[39] D. Tang, B. Liu, R. Niessner, P. Li, D. Knopp, Target-induced displacement reaction accompanying cargo release from magnetic mesoporous silica nanocontainers for fluorescence immunoassay, Anal. Chem. 85 (2013) 10589–10596, https://doi.org/10.1021/ac402713a.
[40] D. Tang, Y. Lin, Q. Zhou, Y. Lin, P. Li, R. Niessner, D. Knopp, Low-cost and highly sensitive immunosensing platform for aflatoxins using one-step competitive displacement reaction mode and portable glucometer-based detection, Anal. Chem. 86 (2014) 11451–11458, https://doi.org/10.1021/ac503616d.
[41] L. Pla, S. Santiago-Felipe, M.Á. Tormo-Mas, J. Pemán, F. Sancenón, E. Aznar, R. Martínez-Máñez, Aptamer-capped nanoporous anodic alumina for Staphylococcus aureus detection, Sens. Actuators B Chem. 320 (2020) 128281, https://doi.org/10.1016/j.snb.2020.128281.
[42] L. Pla, M.C. Martínez-Bisbal, E. Aznar, F. Sancenón, R. Martínez-Máñez, S. Santiago-Felipe, A fluorogenic capped mesoporous aptasensor for gluten detection, Anal. Chim. Acta 1147 (2021) 178–186, https://doi.org/10.1016/j.aca.2020.12.060.
[43] L. Pla, F. Sancenón, M.C. Martínez-Bisbal, C. Bañuls, N. Estañ, M. Botello-Marabotto, E. Aznar, G. Sáez, S. Santiago-Felipe, R. Martínez-Máñez, A new 8-oxo-7,8-2′deoxyguanosine nanoporous anodic alumina aptasensor for colorectal cancer diagnosis in blood and urine, Nanoscale 13 (2021) 8648–8657, https://doi.org/10.1039/d0nr07948k.
[44] Y.H. ElNahass, R.H. Badawy, F.A. ElRefaey, H.A. Nooh, D. Ibrahim, H.A. Nader, H. K. Mahmoud, W.H. ElMetnawy, IDH mutations in AML patients; a higher association with intermediate risk cytogenetics, Asian Pac. J. Cancer Prev. 21 (2020) 721–725, https://doi.org/10.31557/APJCP.2020.21.3.721.
[45] M. Ibáñez, E. Such, J. Cervera, I. Luna, I. Gómez-Seguí, M. López-Pavía, S. Dolz, E. Barragán, O. Fuster, M. Llop, R. Rodríguez-Veiga, A. Avaria, S. Oltra, M. L. Senent, F. Moscardó, P. Montesinos, D. Martínez-Cuadrón, G. Martín, M.A. Sanz, Rapid screening of ASXL1, IDH1, IDH2, and c-CBL mutations in de novo acute myeloid leukemia by high-resolution melting, J. Mol. Diagn. 14 (2012) 594–601, https://doi.org/10.1016/j.jmoldx.2012.06.006.
[46] H. Jiang, X. Ren, X. Cui, J. Wang, W. Jia, Z. Zhou, S. Lin, 1p/19q codeletion and IDH1/2 mutation identified a subtype of anaplastic oligoastrocytomas with prognosis as favorable as anaplastic oligodendrogliomas, Neuro. Oncol. 15 (2013) 775–782, https://doi.org/10.1093/neuonc/not027.
[47] R. Huisgen, 1,3-dipolar cycloadditions. past and future, Angew. Chemie Int. Ed. English 2 (1963) 565–598, https://doi.org/10.1002/anie.196305651.
[48] H.C. Kolb, M.G. Finn, K.B. Sharpless, Click Chemistry, Diverse chemical function from a few good reactions, Angew. Chemie Int. Ed. 40 (2001) 2004–2021, https://doi.org/10.1002/1521-3773(20010601)40:11<2004::AID-ANIE2004>3.0.CO;2-5.
[49] D. Capper, S. Weißert, J. Balss, A. Habel, J. Meyer, D. Jäger, U. Ackermann, C. Tessmer, A. Korshunov, H. Zentgraf, C. Hartmann, A. Von Deimling, Characterization of r132h mutation-specific idh1 antibody binding in brain tumors, Brain Pathol. 20 (2010) 245–254, https://doi.org/10.1111/j.1750-3639.2009.00352.x.
[50] J. Rashidian, R. Copaciu, Q. Su, B. Merritt, C. Johnson, A. Yahyabeik, E. French, K. Cummings, Generation and performance of R132H mutant IDH1 rabbit monoclonal antibody, Antibodies 6 (2017) 22, https://doi.org/10.3390/antib6040022.
[51] S. Takano, W. Tian, M. Matsuda, T. Yamamoto, E. Ishikawa, M.K. Kaneko, K. Yamazaki, Y. Kato, A. Matsumura, Detection of IDH1 mutation in human gliomas: comparison of immunohistochemistry and sequencing, Brain Tumor Pathol. 28 (2011) 115–123, https://doi.org/10.1007/s10014-011-0023-7.

Luis Pla is PhD student at the Polytechnic University of Valencia under the supervision of Prof. Félix Sancenón and Prof. Ramón Martínez-Máñez. He is coauthor of 7 research publications. He is devoted to the development of new probes based on gated materials

Félix Sancenón is full professor at Department of Chemistry at the Polytechnic University of Valencia. He is the coauthor of more than 280 research publications. His current research interest comprises the use of hybrid materials for the development of sensors and for the construction of molecular gates.

M. Carmen Martínez-Bisbal is PhD Assistant Professor at Physical Chemistry Department at the University of Valencia. She is chemist and biochemist. She is coauthor of 48 research publications. Her current research interest comprises the biomarker discovery by NMR spectroscopy and the biomarker sensing involving molecular recognition and electrochemistry.

Ricardo Prat-Acín is PhD Associate Professor of Neurosurgery at Surgery Department at the University of Valencia. Neurosurgeon grade 4 (top) of Spanish professional career at Hospital La Fe of Valencia (Spain). He is double Master in Research and health management and in Management of cancer services. He is coauthor of 43 indexed research publications. His current research interest involves Neurosurgical oncology including awake brain mapping surgery and minimally invasive brain tumor surgery. He is also involved in several multicentric projects related to clinical, and molecular aspects of brain tumors.

Inma Galeano-Senabre is Neurosurgeon grade 4 (top) of Spanish professional career at Hospital La Fe of Valencia (Spain)). She is coauthor of 24 indexed research publications. Her current research interest involves Neurosurgical oncology including awake brain mapping surgery and minimally invasive brain tumor surgery. He is also devoted to the study of brain CSF dynamics.

Marina Botello-Marabotto is PhD student at the Polytechnic University of Valencia under the supervision of Prof. Ramón Martínez-Máñez and Prof. M.Carmen Martínez-Bisbal. She is biotechnologist. She is devoted to the discovery of biomarkers by NMR spectroscopy and to the development of sensors for biomarkers.

Sarai Palanca-Suela, Ph.D., is a specialist Pharmacist in Clinical Biopathology at the University and Polytechnic Hospital La Fe. She is a member of the Clinical and Translational Cancer Research Group (Health Research Institute La Fe) and belongs to the Program of Genetic Counselling in Cancer of the Valencian Community and to the scientific committee of the Valencian biobank network. Her clinical career at the Hospital la Fe has contributed to the implementation of precision medicine in oncology. She is coauthor of 47 research publications and she has participated in national and international congresses (>100), in the development of scientific books (4) and in the direction of master's thesis and PhD students (6). She is also assistant professor at the medical school of the University of Valencia.

Elena Aznar is researcher of the Biomedical Research Networking Center in Bioengineering, Biomaterials and Nanomedicine (CIBER-BBN). She is coauthor of more than 67 research publications. Her current research interest involves the development of smart nanomaterials for controlled release and sensing applications.

Sara Santiago-Felipe is postdoctoral researcher of the Biomedical Research Networking Center in Bioengineering, Biomaterials and Nanomedicine (CIBER-BBN). She is co-author of 14 research publications. Her current research interest involves the development of new sensing materials able to be applied in the biomedical area.

Ramón Martínez-Máñez is full professor at Department of Chemistry at the Polytechnic University of Valencia and also is the director of the Biomedical Research Networking center in Bioengineering, Biomaterials and Nanomedicine (CIBER-BBN). He is the coauthor of more than 510 research publications. His current research interest involves designing gated hybrid materials for on-command delivery applications. He is also involved in developing new sensing methods for different chemicals of interest, especially in the biomedical area.